DALTON
FULL PAPER

Synthesis, structure and magnetic properties of a novel octairon(III) citrate complex †

Isabelle Gautier-Luneau,*[a] Christophe Fouquard,[a] Claire Merle,[a] Jean-Louis Pierre[a] and Dominique Luneau[b]

[a] *Laboratoire de Chimie Biomimétique (LEDSS, UMR CNRS 5616), Université Joseph Fourier, BP 53, 38041, Grenoble cedex 9, France. E-mail: Isabelle.Gautier-Luneau@ujf-grenoble.fr*
[b] *Laboratoire de Chimie Inorganique et Biologique (UMR 5046), CEA-Grenoble, DRFMC, 17, rue des Martyrs, 38054, Grenoble cedex 9, France*

Received 27th February 2001, Accepted 17th May 2001
First published as an Advance Article on the web 3rd July 2001

A novel octairon(III) citrate complex, $(Him)_9[Fe_8(\mu_3\text{-}O)_2(\mu_2\text{-}OH)_2(cit)_6(CH_3CO_2)_2(im)_2](ClO_4)\cdot 13H_2O$ has been obtained from DMF solution, by reacting ferric perchlorate, citric acid and imidazole in a 1 : 1 : 5 ratio. This compound crystallizes in the monoclinic space group $P2_1/n$ with $a = 15.271(1)$, $b = 19.940(1)$, $c = 44.197(1)$ Å, $\beta = 91.965(1)°$, $V = 13450.2(9)$ Å^3 and $Z = 4$. The complex consists of two equivalent tetranuclear units, which are not symmetrically related and are linked together by two of the six tetraionized citrate ligands. The iron(III) ions are antiferromagnetically coupled. Assumption of a four $S = 5/2$ spin system based on $H = -2\Sigma_{i<j} J_{ij}S_iS_j$ leads to satisfactory agreement with the experimental magnetic behavior, with $g = 2.0$ and $J_{13} = J_{23} = -32.1$ cm^{-1}, $J_{12} = J_{14} = -14.5$ cm^{-1}, $J_{24} = J_{34} = -11.1$ cm^{-1}.

Introduction

Ferric citrate plays a paramount role in the iron metabolism of living systems. Citric acid is present in root exudates. It depolymerizes and solubilizes ferric hydroxide, and mobilizes the iron to the membranes of the root cells. It has been shown that *Bradyrhizobium japonicum* 61A152 releases citric acid as a siderophore under iron-deficient growth conditions.[1] Citrate is used as a shuttle to transport ferric iron to the leaves by the xylem sap, and a link between iron metabolism and citrate concentration in plants has been clearly established.[2] *Escherichia coli* possesses one transport system, which is specific for ferric citrate (citrate is in this case an exogenous siderophore that is not formed by the bacteria).[3] In animals (including humans), the non-heme iron in foods enters an exchangeable pool of iron which is not bound to transferrin in blood plasma.[4]

To date, many chemical features of the ferric citrate systems remain undefined.[5] Although the polymeric ferric citrate complex is known,[6] only four discrete iron(III) citrate complexes have been structurally characterized.[7–9] It is clear that the formation of each type of ferric citrate complex depends on the experimental conditions (stoichiometry, solvent, pH, added base, *etc.*). Moreover, in solution, several complexes may be in equilibrium.[10–13] Except for the so-called mononuclear dicitrate complex,[9] which is involved in the citrate transport system of *E. coli*,[3] the biological relevance of any given complex has not been established. We describe in this paper the synthesis, the crystal structure and magnetism of a new octairon(III) citrate complex, $[Fe_8(\mu_3\text{-}O)_2(\mu_2\text{-}OH)_2(cit)_6(CH_3CO_2)_2(im)_2]^{8-}$. This complex is also of interest for comparisons with the nonairon(III) citrate complex recently described by Bino *et al*.[8]

Results and discussion

Synthesis

The novel octanuclear complex has been obtained as the only product in a reproducible manner when following the conditions described in the Experimental section. Nevertheless, in experiments where more concentrated solutions were used, only small green–yellow crystals were obtained corresponding to a dinuclear complex. This dinuclear complex has been identified as $(Him)_2[Fe_2(cit)_2(H_2O)_2]\cdot H_2O\cdot DMF$.[14] It seems that concentrated solutions and fast evaporation lead to the dinuclear species, while more dilute solutions and slow evaporation favor the octanuclear species. These two species could be in equilibrium in DMF solution, in line with what has been suggested for the dinuclear and nonanuclear species in aqueous solution.[8] When pyridine is used instead of imidazole in DMF solution, only a dinuclear species, $(Hpy)_2[Fe_2(cit)_2(H_2O)_2]\cdot 2H_2O$, is obtained. This complex has been previously reported to crystallize in aqueous solution.[7]

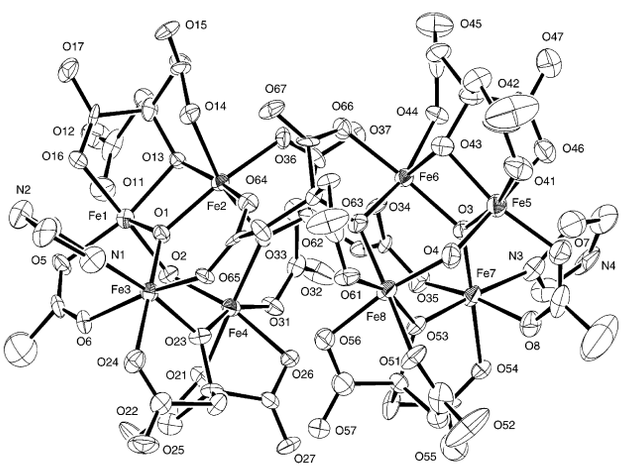

Fig. 1 ORTEP plot of the complex $[Fe_8(O)_2(OH)_2(cit)_6(CH_3CO_2)_2(im)_2]^{8-}$. Ellipsoids are drawn at the 30% probability level.

Structure

The crystal structure reveals a discrete anionic octairon(III) complex, depicted in Fig. 1, involving six tetraionized citrate ligands. The non-coordinated oxygen and nitrogen atoms of the

† Electronic supplementary information (ESI) available: intermolecular distances less than 3.30 Å involving the non-hydrogen atoms. See http://www.rsc.org/suppdata/dt/b1/b101865p/

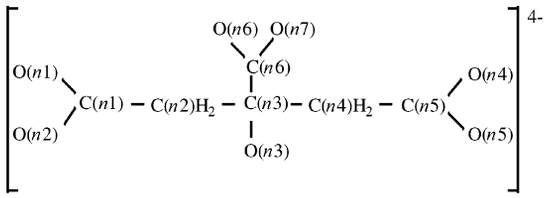

Fig. 2 Numbering scheme for citrate ligand.

Table 1 Selected distances (Å) (with e.s.d.s) in $[Fe_8(O)_2(OH)_2(cit)_6(CH_3CO_2)_2(im)_2]^{8-}$

Atoms	Distance	Atoms	Distance
Fe1–O1	1.982(9)	Fe5–O3	1.94(1)
Fe1–O2	1.963(9)	Fe5–O4	1.97(1)
Fe1–O5	1.96(1)	Fe5–O7	1.98(1)
Fe1–O11	2.03(1)	Fe5–O41	2.08(1)
Fe1–O13	1.945(9)	Fe5–O43	2.010(9)
Fe1–O16	2.04(1)	Fe5–O46	2.04(1)
Fe2–O1	1.939(9)	Fe6–O3	1.961(9)
Fe2–O13	2.040(9)	Fe6–O34	1.99(1)
Fe2–O14	2.058(9)	Fe6–O43	2.02(1)
Fe2–O33	2.047(8)	Fe6–O44	2.04(1)
Fe2–O36	1.991(9)	Fe6–O63	2.04(1)
Fe2–O64	2.01(1)	Fe6–O66	1.991(9)
Fe3–O1	1.84(1)	Fe7–O3	1.865(9)
Fe3–O6	2.07(1)	Fe7–O8	2.03(1)
Fe3–O23	2.041(9)	Fe7–O35	2.03(1)
Fe3–O24	2.08(1)	Fe7–O53	1.98(1)
Fe3–O65	1.99(1)	Fe7–O54	2.05(1)
Fe3–N1	2.12(1)	Fe7–N3	2.14(1)
Fe4–O2	1.940(9)	Fe8–O4	1.96(1)
Fe4–O21	2.09(1)	Fe8–O51	2.09(1)
Fe4–O23	1.99(1)	Fe8–O53	1.973(9)
Fe4–O26	2.066(9)	Fe8–O56	2.04(1)
Fe4–O31	2.00(1)	Fe8–O61	1.98(1)
Fe4–O33	2.004(9)	Fe8–O63	2.020(9)
Fe1–Fe2	3.007(3)	Fe5–Fe6	3.004(3)
Fe1–Fe3	3.405(3)	Fe5–Fe7	3.402(3)
Fe1–Fe4	3.447(3)	Fe5–Fe8	3.486(3)
Fe2–Fe3	3.460(3)	Fe6–Fe7	3.468(3)
Fe2–Fe4	3.542(3)	Fe6–Fe8	3.525(3)
Fe3–Fe4	3.541(3)	Fe7–Fe8	3.514(3)
Fe1–Fe6	8.077(3)	Fe3–Fe8	6.756(3)
Fe1–Fe8	9.070(3)	Fe3–Fe6	7.076(3)
Fe1–Fe7	9.458(3)	Fe3–Fe7	8.090(3)
Fe1–Fe5	10.918(3)	Fe3–Fe5	9.419(3)
Fe2–Fe6	5.160(3)	Fe4–Fe6	6.719(3)
Fe2–Fe8	6.634(3)	Fe4–Fe7	6.878(3)
Fe2–Fe7	7.096(3)	Fe4–Fe8	7.232(3)
Fe2–Fe5	8.068(3)	Fe4–Fe5	9.162(3)

citrate and imidazole ligands of the complex form a three-dimensional hydrogen-bonding network with water molecules and the imidazolium nitrogen atoms. Fig. 2 shows the numbering scheme used for citrate (in which *n* is the number of the citrate and varies between 1 and 6). Selected interatomic distances are listed in Table 1 and angles in Table 2.

The complex consists of two equivalent tetranuclear units linked together by two of the citrate ligands, which are not symmetrically related. Each tetranuclear unit contains two citrate ligands ($n = \{1, 2\}$ and $\{4, 5\}$) coordinated with the same mode of coordination as in the dinuclear complex[7] $[Fe_2(cit)_2(H_2O)_2]^{2-}$, namely, an alkoxo bridge (O*n*3) between two iron atoms (Fe1, Fe2) for $n = 1$, (Fe4, Fe3) for $n = 2$, (Fe5, Fe6) for $n = 4$ and (Fe8, Fe7) for $n = 5$. For each pair of iron atoms, the central (O*n*6) and one terminal carboxylate (O*n*1) are coordinated to the first iron, and the other terminal carboxylate (O*n*4) is coordinated to the second iron. The third citrate of each tetranuclear unit ($n = 3$ and $n = 6$) is coordinated respectively to (Fe2, Fe4) and (Fe6, Fe8) by the alkoxo bridge (O*n*3), the central carboxylate (O*n*6) to one iron, the terminal carboxylate (O*n*1) to the other iron in a monodentate fashion, while the other terminal carboxylate (O*n*4, O*n*5) bridges (in a bis-monodentate fashion) two iron atoms of the other tetranuclear unit (Fe6, Fe7) for $n = 3$ and (Fe2, Fe3) for $n = 6$. This mode of coordination of the citrate ligand binding to four iron atoms has been already observed in the nonairon(III) complex.[8] In the

Table 2 Selected bond angles (°) (with e.s.d.s) in $[Fe_8(O)_2(OH)_2(cit)_6(CH_3CO_2)_2(im)_2]^{8-}$

Atoms	Angle	Atoms	Angle
Fe3–O1–Fe1	125.8(5)	Fe7–O3–Fe5	127.1(5)
Fe2–O1–Fe1	100.2(4)	Fe6–O3–Fe5	100.9(4)
Fe3–O1–Fe2	132.4(5)	Fe7–O3–Fe6	130.0(5)
Fe4–O2–Fe1	124.1(5)	Fe8–O4–Fe5	125.0(6)
Fe1–O13–Fe2	98.0(4)	Fe5–O43–Fe6	96.3(4)
Fe4–O23–Fe3	122.8(5)	Fe8–O53–Fe7	125.7(5)
Fe4–O33–Fe2	121.9(4)	Fe8–O63–Fe6	120.7(4)
O13–Fe1–O2	98.7(4)	O3–Fe5–O4	88.5(4)
O13–Fe1–O5	167.7(4)	O3–Fe5–O7	101.3(4)
O13–Fe1–O1	81.2(4)	O3–Fe5–O43	81.7(4)
O13–Fe1–O11	84.4(4)	O3–Fe5–O46	96.0(4)
O13–Fe1–O16	82.1(4)	O3–Fe5–O41	167.2(4)
O2–Fe1–O5	93.0(4)	O4–Fe5–O7	94.3(5)
O2–Fe1–O1	89.7(4)	O4–Fe5–O43	97.3(4)
O2–Fe1–O11	91.5(4)	O4–Fe5–O46	175.3(5)
O2–Fe1–O16	176.3(4)	O4–Fe5–O41	89.5(5)
O5–Fe1–O1	102.7(4)	O7–Fe5–O43	168.1(5)
O5–Fe1–O11	91.6(4)	O7–Fe5–O46	86.3(5)
O5–Fe1–O16	86.0(4)	O7–Fe5–O41	91.5(5)
O1–Fe1–O11	165.5(4)	O43–Fe5–O46	81.9(4)
O1–Fe1–O16	94.0(4)	O43–Fe5–O41	86.0(4)
O11–Fe1–O16	85.0(4)	O46–Fe5–O41	85.9(5)
O1–Fe2–O36	167.2(4)	O3–Fe6–O34	95.3(4)
O1–Fe2–O64	92.7(4)	O3–Fe6–O66	168.2(4)
O1–Fe2–O13	79.9(4)	O3–Fe6–O43	80.7(4)
O1–Fe2–O33	89.0(4)	O3–Fe6–O44	104.2(4)
O1–Fe2–O14	104.0(4)	O3–Fe6–O63	90.6(4)
O36–Fe2–O64	95.5(4)	O34–Fe6–O66	92.7(4)
O36–Fe2–O13	93.4(4)	O34–Fe6–O43	171.2(4)
O36–Fe2–O33	80.2(4)	O34–Fe6–O44	88.1(4)
O36–Fe2–O14	86.2(4)	O34–Fe6–O63	96.9(4)
O64–Fe2–O13	168.7(3)	O66–Fe6–O43	92.5(4)
O64–Fe2–O33	96.9(4)	O66–Fe6–O44	84.7(4)
O64–Fe2–O14	87.7(4)	O66–Fe6–O63	79.8(4)
O13–Fe2–O33	91.6(3)	O43–Fe6–O44	85.3(4)
O13–Fe2–O14	85.8(4)	O43–Fe6–O63	91.0(4)
O33–Fe2–O14	166.0(4)	O44–Fe6–O63	163.9(4)
O1–Fe3–O65	98.0(4)	O3–Fe7–O53	88.1(4)
O1–Fe3–O23	88.8(4)	O3–Fe7–O8	96.9(4)
O1–Fe3–O6	97.0(4)	O3–Fe7–O35	96.0(4)
O1–Fe3–O24	175.4(4)	O3–Fe7–O54	177.6(4)
O1–Fe3–N1	98.3(4)	O3–Fe7–N3	95.7(5)
O65–Fe3–O23	94.6(4)	O53–Fe7–O8	90.5(4)
O65–Fe3–O6	164.3(4)	O53–Fe7–O35	93.3(4)
O65–Fe3–O24	85.5(4)	O53–Fe7–O54	89.6(4)
O65–Fe3–N1	87.1(4)	O53–Fe7–N3	176.0(5)
O23–Fe3–O6	90.3(4)	O8–Fe7–O35	166.6(4)
O23–Fe3–O24	87.9(4)	O8–Fe7–O54	82.2(4)
O23–Fe3–N1	172.5(5)	O8–Fe7–N3	87.9(5)
O6–Fe3–O24	79.8(4)	O35–Fe7–O54	85.0(4)
O6–Fe3–N1	86.2(4)	O35–Fe7–N3	87.5(4)
O24–Fe3–N1	85.0(4)	O54–Fe7–N3	86.6(5)
O2–Fe4–O23	100.5(4)	O4–Fe8–O53	100.0(4)
O2–Fe4–O31	93.5(4)	O4–Fe8–O61	92.2(4)
O2–Fe4–O33	94.7(4)	O4–Fe8–O63	95.1(4)
O2–Fe4–O26	166.8(4)	O4–Fe8–O56	168.5(4)
O2–Fe4–O21	83.7(4)	O4–Fe8–O51	83.8(4)
O23–Fe4–O31	158.5(4)	O53–Fe8–O61	162.8(4)
O23–Fe4–O33	102.3(4)	O53–Fe8–O63	99.1(4)
O23–Fe4–O26	76.8(4)	O53–Fe8–O56	80.0(4)
O23–Fe4–O21	85.5(4)	O53–Fe8–O51	87.1(4)
O31–Fe4–O33	92.6(4)	O61–Fe8–O63	91.8(4)
O31–Fe4–O26	85.9(4)	O61–Fe8–O56	85.6(4)
O31–Fe4–O21	79.9(4)	O61–Fe8–O51	82.1(4)
O33–Fe4–O26	98.5(4)	O63–Fe8–O56	96.3(4)
O33–Fe4–O21	172.2(4)	O63–Fe8–O51	173.7(4)
O26–Fe4–O21	83.2(4)	O56–Fe8–O51	84.7(4)

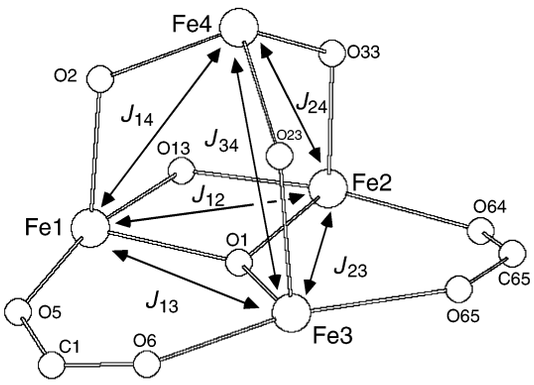

Fig. 3 Scheme of iron(III) bridging ligands with the J exchange integrals in the tetranuclear moiety Fe1 to Fe4, also valid for Fe5 to Fe8.

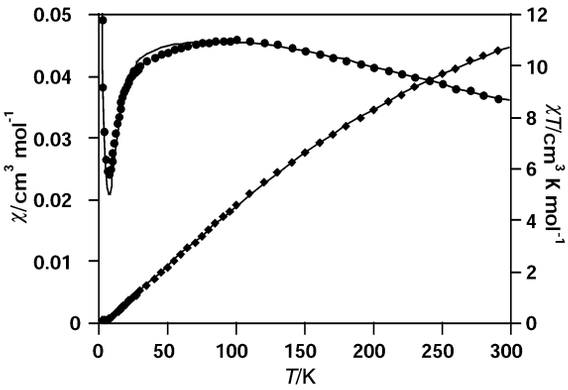

Fig. 4 Temperature dependence of χT (◆) and χ (●) in an applied field of 0.5 T. The calculated curves for $J_{13} = J_{23} = -32.1$ cm^{-1}, $J_{12} = J_{14} = -14.5$ cm^{-1}, $J_{24} = J_{34} = -11.1$ cm^{-1} are shown as solid lines.

octairon(III) complex two citrate ligands are used to connect together two tetranuclear units, while in the nonairon(III) complex, six citrate ligands connect the two terminal units in the molecular "ferric triple decker", to the central one. It is easy to imagine that this mode of coordination may lead to the formation of polynuclear complexes of different sizes. In our case, it can be proposed that a tetranuclear species dimerizes to form the octanuclear complex. Indeed, in the tetranuclear species, one terminal carboxylate should be non-coordinated and will be protonated or deprotonated, depending on the pH of the medium. The non-coordinated carboxylate group has been observed in the dinuclear complex[7] $[Fe_2(citH)_3]^{3-}$ (pH = 3) and in the mononuclear complex[9] $[Fe(cit)_2]^{5-}$ (pH = 8). The versatility of citrate ligand, which is able to coordinate from one to four iron(III) ions, has been reviewed by some of us in detail.[5] Five different modes of coordination have already been characterized. The L/Fe ratio in the complexes varies from 2 to 0.75.

The iron ions are all in a slightly distorted octahedron. Six of them have an $[O_6]$ environment and two have an $[NO_5]$ environment, in which the nitrogen atoms are provided by the imidazole ligands. The oxygen atoms come from the citrate ligands and from two acetate groups, two μ_3-oxo (O1 and O3 atoms) and two μ_2-hydroxo (O2 and O4 atoms). The acetate ligands which were not added in the synthesis process could result from the decomposition of citrate in solution. The cleavage of citrate to acetate and oxaloacetate is a known reaction catalyzed by the enzyme citrate lyase.[15] In our case, it could be a process similar to that found in these enzymatic systems. The oxo and hydroxo oxygens have been assigned considering both the Fe–O distances and angles, and the charge balance in the structure. The Fe–O bond distances range between 1.84(1) and 2.08(1) Å. The shortest distances correspond to Fe–μ_3-oxo bonds and Fe–hydroxo bonds.

The four iron atoms of each tetranuclear unit (Fe1 to Fe4) and (Fe5 to Fe8) form tetrahedra (Fig. 3), in which the octahedra $[FeO_6]$ and $[FeO_5N]$ share vertices or edges, leading to an $\{Fe_4O_5\}$ core. This core shows different iron octahedral stacking from those described by Hagen.[16] The basal plane of the two tetrahedra consists of trinuclear oxo-centered units, (Fe1 to Fe3, μ_3-O1) and (Fe5 to Fe7, μ_3-O3), which are reminiscent of basic iron carboxylate.[17,18] In fact, the nine atoms of the sets (Fe1 to Fe3, O1, O13, O5, O6, O64, O65) and (Fe5 to Fe7, O3, O43, O7, O8, O34, O35) are almost in the same planes with mean deviations from the planes of 0.10 and 0.14 Å, respectively. In the trinuclear oxo-centered units, the iron atoms are doubly bridged. In addition to the μ_3-oxo bridge (μ_3-O1 or μ_3-O3), there is an alkoxo bridge, respectively (μ_2-O13) between Fe1 and Fe2 and (μ_2-O43) between Fe5 and Fe6, leading to the shortest intermetallic distances [3.007(3) and 3.004(3) Å] in the complex. There is one carboxylate bridge (O64–C65–O65) between Fe2 and Fe3 and (O34–C35–O35) between Fe6 and Fe7, and one acetate bridge (O5–C1–O6) between Fe1 and Fe3 and (O7–C3–O8) between Fe5 and Fe7. In each tetrahedron (Fe1 to Fe4) and (Fe5 to Fe8), the three iron atoms of the basal plane are connected to the fourth (Fe4 or Fe8) by two alkoxo bridges (μ_2-O23 between Fe4 and Fe3 and μ_2-O33 between Fe4 and Fe2; μ_2-O53 between Fe8 and Fe7 and μ_2-O63 between Fe8 and Fe6) and one hydroxo bridge (μ_2-O2 between Fe4 and Fe1; μ_2-O4 between Fe8 and Fe5) (Fig. 3).

The intermetallic distances in the tetrahedra range between 3.007(4) and 3.541(3) Å for Fe1 to Fe4, and between 3.004(3) and 3.525(3) Å for Fe5 to Fe8, while the intermetallic distances between the tetranuclear units are between 5.160(3) and 10.918(3) Å. The shortest distance [5.160(3) Å] is observed between Fe2 and Fe6, which are doubly linked by the two citrate ligands connecting the two tetranuclear units. This distance is shorter than the corresponding distance in the nonairon complex, in which the approximate distance between two trinuclear units connected in the same fashion, by three citrate ligands, is 5.6 Å.

Magnetic behavior

The magnetic behavior of the complex is shown in Fig. 4 in the form of the temperature dependence of the molar magnetic susceptibility χ and its product with temperature χT. At room temperature, χT is 10.8 cm^3 K mol^{-1}, which is much lower than the expected value of 35 cm^3 K mol^{-1} for eight non-interacting Fe(III) ions. χT falls to zero at 2 K while the χ *vs.* T curve shows a rounded maximum around 100 K. The increase of χ below 6 K is attributed to a small amount of paramagnetic impurity.

This magnetic behavior implies that strong antiferromagnetic couplings occur between the Fe(III) ions, which may result in a $S = 0$ ground state. Owing to the crystal structure (*vide infra*), this octanuclear compound must, in fact, be viewed as the cumulative contribution of the two non-interacting tetranuclear units (Fe1 to Fe4) and (Fe5 to Fe8). Indeed, the bridging between the two units is not expected to mediate significant exchange coupling interactions (Fig. 1). Accordingly, the temperature dependence of the magnetic susceptibility was analyzed by a refinement program[19] which numerically diagonalizes the isotropic Hamiltonian ($H = -2\Sigma_{i<j}J_{ij}S_iS_j$), assuming four $S = 5/2$ spins with six J_{ij} ($i < j \leq 4$) exchange coupling constants in between (Fig. 3) and keeping g at 2.

A first attempt to fit the experimental data considering all six Fe–Fe interactions as equal ($J_{12} = J_{13} = J_{14} = J_{23} = J_{24} = J_{34}$) was unsuccessful, as might be expected owing to the low symmetry of the complex. In both tetranuclear cores, three of the Fe(III) ions (Fe1 to Fe3 and Fe5 to Fe7) are μ_3-oxo and carboxylate-bridged to each other in an Fe_3O arrangement, reminiscent of basic iron carboxylate.[17,18] Each of these three Fe(III) ions interacts additionally with the fourth (Fe4 or Fe8) through a single alkoxo or hydroxo bridge. From previous results on basic iron carboxylate,[18] alkoxo-bridged polyiron(III)[20] and

Table 3 Correlation between structural parameters (P/Å) and exchange coupling (J/cm^{-1})

	P^a	J^b	J^c	$J_{calc}{}^d$
Fe1–Fe3	1.91	−27.5	−31.4	−32.1
Fe2–Fe3	1.89	−35.4	−37.8	−32.1
Fe5–Fe7	1.90	−31.2	−34.4	−32.1
Fe6–Fe7	1.91	−27.5	−31.4	−32.1
Fe1–Fe2	1.96	−14.6	−19.7	−14.5
Fe1–Fe4	1.95	−16.5	−21.6	−14.5
Fe5–Fe6	1.95	−16.5	−21.6	−14.5
Fe5–Fe8	1.97	−12.8	−18.0	−14.5
Fe2–Fe4	2.03	−6.0	−10.3	−11.1
Fe3–Fe4	2.02	−6.8	−11.3	−11.1
Fe7–Fe8	1.98	−11.3	−16.4	−11.1
Fe6–Fe8	2.03	−6.0	−10.3	−11.1

[a] P is defined as half the shortest pathway between two bridged Fe(III) ions. [b] $J = -A\exp(BP)$; ref. 21, $A = 8.763 \times 10^{11}$, $B = -12.663$. [c] $J = -A\exp(BP)$; ref. 22, $A = 1.625 \times 10^{9}$, $B = -9.3$. [d] From the fitting of this experimental data.

nonairon(III)[8] complexes, it might be expected that the magnitude of the antiferromagnetic coupling in the Fe_3O moieties (Fe1 to Fe3 and Fe5 to Fe7) would depart markedly from those with the fourth. In this regard, the use of only two sets of interactions ($J_{12} = J_{13} = J_{23} \neq J_{14} = J_{24} = J_{34}$) did not allow the fitting of the experimental data. Finally, an acceptable fit was obtained, as shown by the solid lines in Fig. 4, when taking into account three sets of interactions ($J_{13} = J_{23} = -32.1$ cm^{-1}, $J_{12} = J_{14} = -14.5$ cm^{-1}, $J_{24} = J_{34} = -11.1$ cm^{-1}). An additional weighted paramagnetic impurity of 1.6 mol percent for an $S = 5/2$ species, was also introduced in the refinement process, as suggested by the increase in the magnetic susceptibility at low temperature (Fig. 4). This result is consistent with the structure, considering the different magnetic superexchange pathways. Indeed, in both tetranuclear units, two operate through a μ_3-oxo and a carboxylate (Fe1, Fe3; Fe2, Fe3; Fe5, Fe7; Fe6, Fe7), one through a μ_3-oxo and an alkoxo bridge (Fe1, Fe2; Fe5, Fe6), one is a single hydroxo bridge (Fe1, Fe4; Fe5, Fe8) and two *via* a single alkoxo bridge (Fe3, Fe4; Fe2, Fe4; Fe6, Fe8; Fe7, Fe8). Increasing the number of independent interactions did not improve the fit of the experimental data. It should be stressed that the refinement process takes into account only four $S = 5/2$ spins, but applies to the octanuclear complex. So the above antiferromagnetic exchange coupling constants must be considered as mean values for the couplings in each tetranuclear core. Indeed, while they show a similar arrangement, the two tetranuclear cores (Fe1 to Fe4) and (Fe5 to Fe8) are not symmetry related and exhibit slight differences in angles and bond lengths which may induce small differences in exchange coupling strength. However, as shown in Table 3, the magnitude of the above magnetic interactions compares well with those calculated from empirical correlation[21,22] between the strength of the exchange coupling (J) and the average Fe–O distance (P), defined as half the shortest superexchange pathway.

Experimental

Synthesis of (Him)$_9$[Fe$_8$(μ_3-O)$_2$(μ_2-OH)$_2$(cit)$_6$(CH$_3$CO$_2$)$_2$(im)$_2$](ClO$_4$)·13H$_2$O

Commercial reagents and solvents were used as obtained, without further purification. A solution of 130 mg (0.25 mmol) of ferric perchlorate Fe(ClO$_4$)$_3$·9H$_2$O in DMF (2 mL), was added at room temperature, to a stirred solution of 48 mg (0.25 mmol) of citric acid (C$_6$H$_8$O$_7$) in DMF (3 mL). To the resulting yellow solution was then added imidazole (1.25 mmol), previously solubilized in 5 mL of DMF. The solution turned orange–red and was filtered to eliminate any precipate which formed. Small orange crystals, which were used for the X-ray diffraction and magnetic studies, were grown after 2 months of slow evaporation (yield, 15%). Anal. calc. for C$_{73}$H$_{111}$N$_{22}$O$_{67}$ClFe$_8$: C, 30.75; H, 3.92; N, 10.81; Cl, 1.24; Fe, 15.67; found: C, 31.16; H, 3.94; N, 11.14; Cl, 1.19; Fe, 15.96%.

CAUTION: suitable care and precautions should be taken when handling perchlorate salts.

Table 4 Crystallographic experimental details for (Him)$_9$[Fe$_8$(O)$_2$(OH)$_2$(cit)$_6$(CH$_3$CO$_2$)$_2$(im)$_2$](ClO$_4$)·13H$_2$O

Formula	C$_{73}$H$_{111}$O$_{67}$N$_{22}$ClFe$_8$
Fw	2851.02
Crystal system	Monoclinic
Space group	$P2_1/n$
a/Å	15.271(1)
b/Å	19.940(1)
c/Å	44.197(1)
β/°	91.965(1)
V/Å^3	13450.2(9)
Z	4
μ/mm^{-1}	0.50
λ(Ag-K$_\alpha$)/Å	0.5608
$R(F)$	0.1075
$Rw(F)$	0.1302
S	1.97
$\Delta\rho_{max}$/e Å^{-3}	0.92
$\Delta\rho_{min}$/e Å^{-3}	−0.68

$R(F) = \Sigma||F_o|-|F_c||/\Sigma|F_o|$, $Rw(F) = [\Sigma(|F_o|-|F_c|)^2/\Sigma wF_o^2]^{1/2}$, $w = 1/[\sigma^2(F_o) + 2.5 \times 10^{-3}|F_o|]$.

X-Ray crystallography

Crystallographic experimental details for the octairon complex are given in Table 4. Data were collected at 293 K for 2 days on a small orange platelet. The crystal (0.2 × 0.1 × 0.05 mm) was closed in a capillary tube on a Kappa CCD Nonius diffractometer equipped with graphite monochromatized Ag-Kα radiation. The crystal to detector distance was 50 mm. The CCD data collection was carried out by the rotation technique: 180 successive images of 1° range each were recorded about the vertical phi axis, with the CCD detector perpendicular to the beam direction. Each image was collected twice in order to correct for "zingers". The CCD images were treated by using the Denzo-SMN software.[23] The 43278 collected Bragg reflections were indexed, integrated and averaged in the $P2_1/n$ space group, with R_{sym} values of 0.08, with 10922 independent reflections.

The structure was solved using an automatic Patterson procedure and refined using TEXSAN software.[24] All non-hydrogen atoms were refined with anisotropic thermal parameters. For the hydrogen atoms, only those of the citrate, acetate and imidazole ligands were introduced in the refinement process, in idealized positions riding on the carrier atoms with isotropic thermal parameters. In the lattice, there is one perchlorate anion and nine independent imidazolium (Him$^+$) cations. Three imidazolium cations were refined with isotropic thermal parameters, the other six and the perchlorate anion were refined with anisotropic thermal parameters. Seventeen oxygen atoms of water molecules of crystallization were localized from the Fourier difference maps, of which eight were refined with a half-occupancy, corresponding to thirteen water molecules in the formula. The final cycle refinement, including 1391 parameters, converged to $R(F) = 0.107$ [for 7470 $F > 1.5\sigma(F)$], $Rw(F) = 0.130$ and goodness-of-fit $S = 1.97$.

CCDC reference number 163033.

See http://www.rsc.org/suppdata/dt/b1/b101865p/ for crystallographic data in CIF or other electronic format.

Magnetic susceptibility measurements

The magnetic susceptibilities were measured in the 2–300 K temperature range with a Quantum Design MPMS superconducting SQUID magnetometer operating at a field strength

of 0.5 T. The data were corrected for the diamagnetism of the constituent atoms using Pascal constants.

Acknowledgements

We thank Pierre Bordet (Laboratoire de Cristallographie, CNRS, Grenoble, France) for the data collection on the Kappa CCD Nonius diffractometer.

References

1 M. L. Guerinot, E. J. Meidl and O. Plessner, *J. Bacteriol.*, 1990, **172**, 3298.
2 A. Pich, G. Scholz and K. Seifert, *J. Plant Physiol.*, 1991, **137**, 323.
3 M. Ochs, S. Veitinger, I. Kim, Q. Welz, A. Angerer and V. Braun, *Mol. Microbiol.*, 1995, **5**, 119.
4 M. Grootveld, J. D. Bell, B. Halliwell, O. I. Aruoma, A. Bomford and P. J. Sadler, *J. Biol. Chem.*, 1989, **264**, 4417.
5 J. L. Pierre and I. Gautier-Luneau, *Biometals*, 2000, **13**, 91.
6 T. G. Spiro, G. Bates and P. Saltman, *J. Am. Chem. Soc.*, 1967, **89**, 5559.
7 I. Shweky, A. I. Bino, D. P. Goldberg and S. J. Lippard, *Inorg. Chem.*, 1994, **23**, 5161.
8 A. I. Bino, I. Shweky, S. Cohen, E. R. Bauminger and S. J. Lippard, *Inorg. Chem.*, 1998, **37**, 5168.
9 M. Matzapetakis, C. P. Raptopoulou, A. Tsohos, V. Papaefthymiou, N. Moon and A. Salifoglou, *J. Am. Chem. Soc.*, 1998, **120**, 13266.
10 C. F. Timberlake, *J. Chem. Soc.*, 1964, 5078.
11 T. B. Fields, J. L. McCourt and W. A. E. McBride, *Can. J. Chem.*, 1974, **52**, 3119.
12 R. B. Martin, *J. Inorg. Biochem.*, 1986, **28**, 181.
13 H. Yokoi, T. Mitani, Y. Mori and S. Kawata, *Chem. Lett.*, 1994, 281.
14 I. Gautier-Luneau, C. Merle, C. Fouquard and J. L. Pierre, unpublished results.
15 R. B. Wheat and S. J. Ajl, *J. Biol. Chem.*, 1955, **217**, 897; R. B. Wheat and S. J. Ajl, *J. Biol. Chem.*, 1955, **217**, 909; R. J. Harvey and E. B. Collins, *J. Biol. Chem.*, 1963, **238**, 2648.
16 K. S. Hagen, *Angew. Chem., Int. Ed. Engl.*, 1992, **31**, 1010.
17 S. M. Oh, D. N. Hendrickson, K. L. Hassett and R. E. Davis, *J. Am. Chem. Soc.*, 1984, **106**, 7984; S. M. Oh, D. N. Hendrickson, K. L. Hassett and R. E. Davis, *J. Am. Chem. Soc.*, 1985, **107**, 8009; S. M. Oh, S. R. Wilson, D. N. Hendrickson, S. E. Woehler, R. J. Wittebort, D. Inniss and C. E. Strouse, *J. Am. Chem. Soc.*, 1987, **109**, 1063; S. M. Oh, S. R. Wilson, D. N. Hendrickson, S. E. Woehler, R. J. Wittebort, D. Inniss and C. E. Strouse, *J. Am. Chem. Soc.*, 1987, **109**, 1073; T. Sato, F. Ambe, K. Endo, M. Katada, H. Maeda, T. Nakamoto and H. Sano, *J. Am. Chem. Soc.*, 1996, **118**, 3450; C. E. Anson, J. P. Bourke, R. D. Cannon, U. A. Jayasooriya, M. Molinier and A. K. Powell, *Inorg. Chem.*, 1997, **36**, 1265; T. Nakamoto, M. Hanaya, M. Katada, K. Endo, H. Kitagawa and H. Sano, *Inorg. Chem.*, 1997, **36**, 4347; C. C. Wu, S. A. Hunt, P. K. Gantzel, P. Gütlich and D. N. Hendrickson, *Inorg. Chem.*, 1997, **36**, 4717.
18 E. M. Holt, S. L. Holt, W. F. Tucker, R. O. Asplund and K. J. Watson, *J. Am. Chem. Soc.*, 1974, **96**, 2621; S. M. Gorun and S. J. Lippard, *J. Am. Chem. Soc.*, 1985, **107**, 4571; S. M. Gorun, G. C. Papaefthymiou, R. B. Frankel and S. J. Lippard, *J. Am. Chem. Soc.*, 1987, **109**, 4244.
19 E. Belorizky, P. H. Fries, E. Gojon and J. M. Latour, *Mol. Phys.*, 1987, **61**, 661. Details on the diagonalization program can be obtained on request from fries@drfmc.ceng.cea.fr.
20 A. Caneschi, A. Cornia, A. C. Fabretti, D. Gatteschi and W. Malavasi, *Inorg. Chem.*, 1995, **34**, 4660; S. Parsons, G. A. Solan and R. E. P. Winpenny, *J. Chem. Soc., Chem. Commun.*, 1995, 1987; G. L. Abbati, A. Cornia, A. C. Fabretti, W. Malavasi, L. Schenetti, A. Caneschi and D. Gatteschi, *Inorg. Chem.*, 1997, **36**, 6443.
21 S. M. Gorun and S. J. Lippard, *Inorg. Chem.*, 1991, **30**, 1625.
22 D. Gatteschi, A. Caneschi, R. Sessoli and A. Cornia, *Chem. Soc. Rev.*, 1996, 101.
23 Z. Otwinowski and W. Minor, *Processing of X-Ray Diffraction Data Collected in Oscillation Mode*, in *Methods in Enzymology, Volume 276: Macromolecular Crystallography*, ed. C. W. Carter, Jr. and R. M. Sweet, Academic Press, 1997, part A, pp. 307–326.
24 TEXSAN, Single Crystal Structure Analysis Software, version 1.7, Molecular Structure Corporation, 3200 Research Forest Drive, The Woodlands, TX 77381, USA, 1995.